Endoscopic image analysis of photosensitizer fluorescence as a promising noninvasive approach for pathological grading of bladder cancer *in situ*

James Chen Yong Kah
National University of Singapore
Division of Bioengineering
7 Engineering Drive 1
Singapore 117574

Weber Kam On Lau
Singapore General Hospital
Department of Urology
Outram Road
Singapore 169608

Phuay Hoon Tan
Singapore General Hospital
Department of Pathology
Outram Road
Singapore 169608

Colin James Richard Sheppard
National University of Singapore
Division of Bioengineering
7 Engineering Drive 1
Singapore 117574

Malini Olivo
National Cancer Centre Singapore
Division of Medical Sciences
11 Hospital Drive Singapore 169610
and
Singapore Bioimaging Consortium
Bio-optical Imaging
11 Biopolis Street #02-02 Helios
Singapore 138667
and
National University of Singapore
Department of Pharmacy
Block S4, 18 Science Drive 4
Singapore 117543

Abstract. Our aim is to apply image analysis on photosensitizer fluorescence and compare the relationship between histopathology and endoscopic fluorescence imaging. The correlation between hypericin fluorescence and histopathology of diseased tissue was explored in a clinical study involving 58 fluorescence cystoscopic images from 23 patients. Based on quantification of fluorescence colorimetric parameters extracted from the image analysis, diagnostic functions were developed to pathologically classify the bladder cancer. Our preliminary results show that the differences in fluorescence intensity ratios among the three different grades of bladder cancer are statistically significant. The results also show a decrease in macroscopic fluorescence intensity that correlated with higher cancer grades. By combining both the red-to-green and red-to-blue fluorescence intensity ratios into a 2-D scatter plot and defining diagnostic linear discrimination functions on the data points, this technique is able to yield an average sensitivity and specificity of around 68.6% and 86.1%, respectively, for pathological cancer grading of the three different grades of bladder cancer in our study. We conclude that our proposed approach in applying colorimetric intensity ratio analysis on hypericin fluorescence shows potential to optically grade bladder cancer *in situ*. [DOI: 10.1117/1.2981827]

Keywords: photodynamic diagnosis; fluorescence diagnostic imaging; photosensitizer; hypericin; bladder cancer; image analysis; histopathology; fluorescence cystoscopy.

Paper 08044RR received Feb. 3, 2008; revised manuscript received Apr. 29, 2008; accepted for publication May 9, 2008; published online Sep. 22, 2008.

1 Introduction

Bladder cancer is the sixth most common form of malignancy worldwide, accounting for 4% of all cancer cases.[1] Bladder cancer patients usually suffer from high recurrence, progression, and mortality rates.[2,3] The survival and treatment option of the bladder cancer patient is related to the different stages and grades of malignancies detected. Therefore, accurate pathological diagnosis of bladder cancer will allow rational selection of treatment, which is crucial to reduce its recurrence, progression, and mortality rates. The current methods of surveillance of patients suspected of bladder cancer or who are at high risk of recurrent bladder cancer are regular white-light cystoscopy followed by random cold-cup biopsies on suspicious sites and *ex vivo* histological examination of the tissue to stage and grade the bladder cancer. Conventional histopathological examination is currently the gold standard for assessing the pathological status of a suspicious lesion or growth. This approach to diagnose bladder cancer presents at least four major limitations: First, although noninvasive papillary tumors are visible under white-light cystoscopy, early flat lesions such as dysplasia and carcinoma *in situ* (CIS) are hardly visible,[4] especially if the bladder is overdistended and trabeculated or there is ongoing cystitis. These flat neoplastic lesions are found to have a significant impact on the recur-

Address all correspondence to: Malini Olivo, National Cancer Centre Singapore, Division of Medical Science, 11 Hospital Drive, Singapore 169610. Tel: (65) 64368317; Fax: (65) 63213606; E-mail: dmsmcd@nccs.com.sg

1083-3668/2008/13(5)/054022/9/$25.00 © 2008 SPIE

rence and progression rates of bladder cancer.[5] Second, histological analysis requires tissue removal, i.e., biopsy, and diagnostic accuracy can be compromised by random sampling and handling of specimens. Due to the randomness of biopsy, there is a risk that the biopsy will miss the intended lesion and be falsely negative.[6] Also, tissue sampling may not always adequately represent the biochemical or pathological process under investigation because of tissue heterogeneity, which is especially characteristic of most tumors.[7] Third, tissue biopsy presents its associated risks, along with delay, expense, and psychological trauma to patients. Last, histopathology cannot provide immediate diagnostic feedback to the patient.

To overcome these shortcomings, optical imaging techniques such as light-induced fluorescence (LIF) endoscopy have been developed with the potential of performing noninvasive "optical biopsies" to detect and diagnose cancer *in vivo*. The principle behind this technique is based on the detection of endogenous tissue autofluorescence[8–10] or the exogenous fluorescence of dyes selectively accumulated in tumor tissue.[11–13] LIF techniques could reduce the risk of physical biopsies by decreasing the number of biopsies or even replacing them altogether.[14] Photodynamic diagnosis (PDD) is a widely reported LIF endoscopy technique using photosensitive fluorescence dyes called photosensitizers that selectively detect and label suspicious lesions. We have previously demonstrated the use of fluorescence cystoscopy using photosensitizers such as 5-aminolevulinic acid (5-ALA) and hypericin to improve the detection of flat lesions in bladder carcinoma.[4,15,16] Besides the improved detection of flat lesions [89.1% for 5-ALA (Ref. 4) and 93% for hypericin[17,18] versus 65.6% for white light[4]], the increase in sensitivity compared to white-light cystoscopy has led to their application in fluorescence-guided biopsies to reduce the number of unnecessary biopsies, thereby reducing the risk of complications from these additional biopsies. Despite these encouraging results, photosensitizers usually suffer from modest specificity in fluorescence labeling to result in a high amount of false positives.[4,19–21] Also, without proper objective fluorescence quantification, the decision of what is considered fluorescence positive or negative is made by clinicians based on their subjective visual impression, thus further adding to the false-positive results. Various groups have attempted to address the problems described have through the application of digital image analysis to objectively quantify the fluorescence intensity of these fluorescence images and have reported promising results in increased specificity.[22,23] However, even with improved specificity in tumors and reduced number of unneccessary biopsies, the laborious task of histopathological sample preparation and analysis is still required for further staging and grading of tumor.

In this study, we investigate the possibility of using the fluorescence from the photosensitizer hypericin to pathologically grade transitional cell carcinoma (TCC) of the bladder *in situ* by applying image analysis on its fluorescence characteristics. Hypericin has been widely demonstrated as a selective marker of bladder cancer with high sensitivity and specificity compared to other commonly used photosensitizers such as ALA and ALA esters.[16–18] It is found to be safe for clinical use without any adverse side effects, and it also showed no genotoxic and cytotoxic results either *in vitro* or *in vivo*.[15,24,25] We hypothesize that hypericin can function as a fluorescent probe for certain biochemical, molecular, or phenotypic markers in cells and tissue that are differentially expressed with different grades of TCC. We based our hypothesis from the results of our previous *in vitro* studies on microscopic fluorescence characteristics of hypericin that showed differential fluorescence staining with different grades of bladder carcinoma cell lines.[16] These results have indicated the potential in exploiting hypericin fluorescence for grading of bladder cancer and thus served as a basis for extending our microscopic fluorescence analysis to macroscopic cystoscopic images. The outcome of this study might present a novel alternative to routine histopathology involving tissue biopsies and laborious histological analysis to diagnose the grade of bladder cancer.

2 Materials and Methods

2.1 *Patient Selection*

Twenty-three patients (18 men and 5 women) with a mean age of 65.0 years (range 46 to 81 years) who are suspected of primary or recurrent bladder cancer were enrolled for this clinical study at the Singapore General Hospital with no exclusion criteria, following their informed consent. Fifty-eight hypericin fluorescence cystoscopic images were obtained from these patients, together with their corresponding histopathological status from biopsy specimens taken from the same imaging site. The diagnosis based on histopathology was used as the gold standard for classifying the images into the various grades of cancer. This study was reviewed and approved by the Ethics Committee of the Singapore General Hospital and National Cancer Centre Singapore.

2.2 *Fluorescence Cystoscopy*

Patients were administered with hypericin via intravesical instillation into the bladder, followed by an *in situ* incubation period of 2 h in the bladder. The bladder instillation solution was prepared from 16 mM hypericin dissolved in absolute ethanol, diluted 1,000-fold in a 1% plasma protein solution in buffered saline and filtered with a sterile membrane. Aliquots of 25 ml were then kept frozen until use and 25 ml saline was added to obtain a 50-ml instillation solution containing 8 μM hypericin. A preliminary study on patients with papillary superficial Ta disease had shown that this was the preferred concentration and volume for adequate hypericin fluorescence.[16] The patients were advised to change their position at regular intervals so that the hypericin was well distributed in the bladder tissue. After the incubation period, the bladder was emptied, and fluorescence cystoscopy was performed swiftly on the patient's bladder under excitation with blue light (370 to 450 nm) to minimize any possibilities of hypericin photobleaching. Biopsies of suspicious red fluorescent regions and surrounding nonfluorescent regions were taken from the imaged tissue sites and sent for routine histopathology to obtain the tissue histological classification for the corresponding fluorescence images.

2.3 *Instrumentation*

The digitized fluorescence endoscopic imaging system used in this study was previously described in detail, and its schematic is shown in Fig. 1.[26] Briefly, the system consists of an illumination console, a fluorescence detection unit, a video

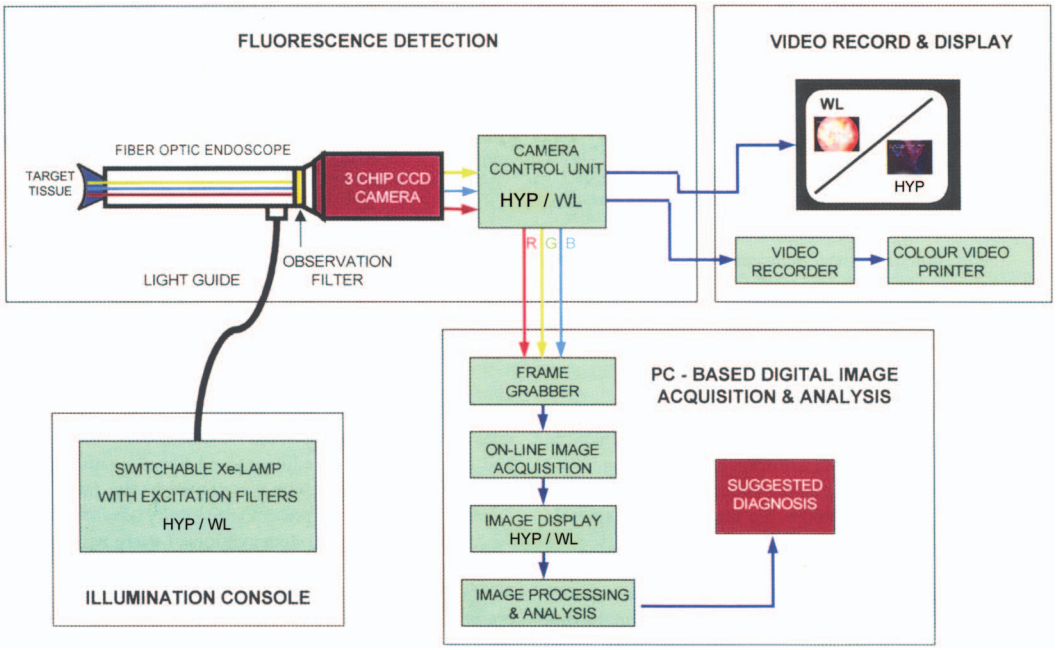

Fig. 1 Schematic diagram of the digitized fluorescence endoscopy imaging system for early cancer diagnosis. WL mode—white light illumination mode; HYP mode—hypericin fluorescence excitation mode.

displaying and recording unit, and a computer system for image acquisition, display and processing. A 100-W xenon short arc lamp (D-Light AF system, Karl Storz, Germany) was used for both the white-light illumination and the hypericin fluorescence excitation when filtered by a bandpass filter (370 to 450 nm). The irradiance of the blue light at the cystoscope tip was approximately 50 mW/cm^2. Both illumination and observation of tissue of interest were achieved via a modified cystoscope integrated with an optical long-pass filter in the cystoscopic eyepiece with cutoff wavelength at 470 nm that transmits only 8% of the diffusely backscattered excitation blue light from the tissue but over 98% of light in the 470 to 800-nm range. This minimizes the backscattered blue excitation light while allowing the red hypericin fluorescence to pass through the cystoscope efficiently.[27] The fluorescence images were detected by a sensitive three-chip color CCD video camera with a pixel resolution of 768×592 (Tricam SL-PDD, Karl Storz, Tuttlingen, Germany), connected to the modified cystoscope with its RGB video outputs fed simultaneously to a frame grabber (Matrox Genesis-LC) at a rate of 25 frames per second for capturing and digitizing the images. The digitized images were stored for offline image processing, and the processed image can be displayed on the computer screen in near real time for further analysis and diagnosis.

2.4 *Image Analysis*

An image processing routine was developed from the Olympus MicroImage 4.0 (Media Cybernetics) software to carry out the various processing, including contrast enhancement, histogram thresholding, and segmentation, prior to the colorimetric analysis, as shown in Fig. 2. The image contrast was first enhanced by histogram equalization, i.e., stretching the image histogram to fill all 256 levels of the 8-bit image, after which the histogram for the hue was extracted for the entire image. This global histogram will typically be bimodal, with two peaks in the hue, one attributed to the normal blue background and the other peak attributed to the red fluorescence from the suspicious lesion. A threshold between the two peaks was then determined by finding the minimum point between the two modes to define the range of hue values to be considered at suspicious against the rest of the normal background. Hue values above the threshold (red region) were considered in the area of interest (AOI). An AOI based on such hue segmentation of lesion area in the cystoscopic images was then defined to segment the suspicious lesion area out from the rest of the background image. The fluorescence intensities of the red, blue, and green channels of the fluorescence images within the AOI were then extracted and quantified. We note that no saturation in the intensity was observed for any of the three color channels, which may affect the results. Intensity ratios were calculated from the three colorimetric parameters to get the red-to-green intensity ratio (I_R/I_G) and the red-to-blue intensity ratio (I_R/I_B) within the AOI. Statistical averages of the intensity ratios for all the patient images under each histological classification were then calculated and compared with histopathological status of the imaged sites to ascertain any correlation. The possible changes in the intensity ratios with the observation distance between the tip of the endoscope and the tissue had previously been reported by our group.[22,23] Despite the decreased fluorescence intensity with increasing imaging distance, the intensity ratios I_R/I_G and I_R/I_B remained nearly consistent in the normal tissue or in the tumor. We noted that the intensity ratios were also independent of the observation geometry and the fluctuation of the excitation irradiance, since all three color channels depend on the distance, angles of the irradiation and observation, and the tissue optical properties in a similar manner. The intensity

ratios thus form a robust diagnostic algorithm for cancer grading in this study.

2.5 *Statistical and Histopathological Analysis*

In assessing the pathological status, the histopathological results were regarded as the gold standard. The tumors were graded by a central pathologist unaware of origin, using the international systems for urothelial neoplasia. In this study, hypervascularized, erythematous, erosive, or edematous areas of the mucosa were considered nonspecific inflammation of the bladder mucosa. Normal, inflammation, and hyperplasias were classified as benign conditions. All three grades of invasive TCC, i.e., grades I, II, and III were classified as malignant pathological changes. The unpaired two-sided Student's *t*-test was performed on the fluorescence intensity ratios I_R/I_G and I_R/I_B to determine whether they were statistically significant for discriminating malignant from benign tissue and the one-way ANOVA test with one-way analysis of variance was performed on the fluorescence intensity ratios I_R/I_G and I_R/I_B to determine whether they were statistically significant for discriminating between the multiple groups, i.e., normal, inflammatory hyperplasia, and three different grades of TCC. The sensitivity and specificity of using hypericin fluorescence for grading the bladder cancer *in situ* were also determined as defined here[4]:

$$\text{Sensitivity} = \frac{TP}{TP + FN}, \quad \text{Specificity} = \frac{TN}{TN + FP},$$

where TP=true positive, TN=true negative, FP=false positive, and FN=false negative.

Table 1 Histopathological classification of the 58 cystoscopic images used in this study.

Pathology	Number of Lesions (%)
Normal	10 (17.2)
Inflammation and hyperplasia	12 (20.7)
Grade I TCC	11 (19.0)
Grade II TCC	13 (22.4)
Grade III TCC	12 (20.7)
Total	**58** (**100.0**)

3 Results and Discussion

3.1 *Patient Classification and Side Effects*

Overall, 58 cystoscopic images from 23 patients were taken from various sites of the bladder in which, after histopathological confirmation, 10 were found to be normal, 12 hyperplasias with inflammation, 11 grade I TCC, 13 grade II TCC, and 12 grade III TCC. The breakdown of histopathological status of the cystoscopic images is summarized in Table 1. All 23 patients involved in this study were subjected to intravesical instillation of hypericin. One major advantage of intravesical instillation of hypericin is that it is topical and therefore avoids the intravenous route and systemic side effects such as cutaneous adverse photoreactions due to photosensitivity. There were no reports of skin photosensitization or other side effects found in patients who have undergone hypericin fluorescence cystoscopy. There are also no reports of phototoxic-

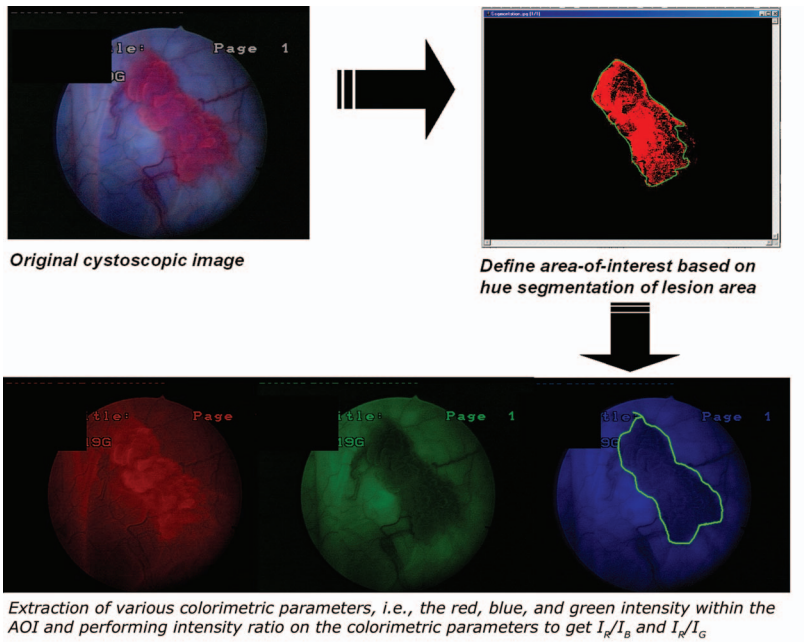

Fig. 2 Schematics of the algorithm used in fluorescence image processing to extract the three colorimetric parameters and hence obtain the two diagnostic intensity ratios.

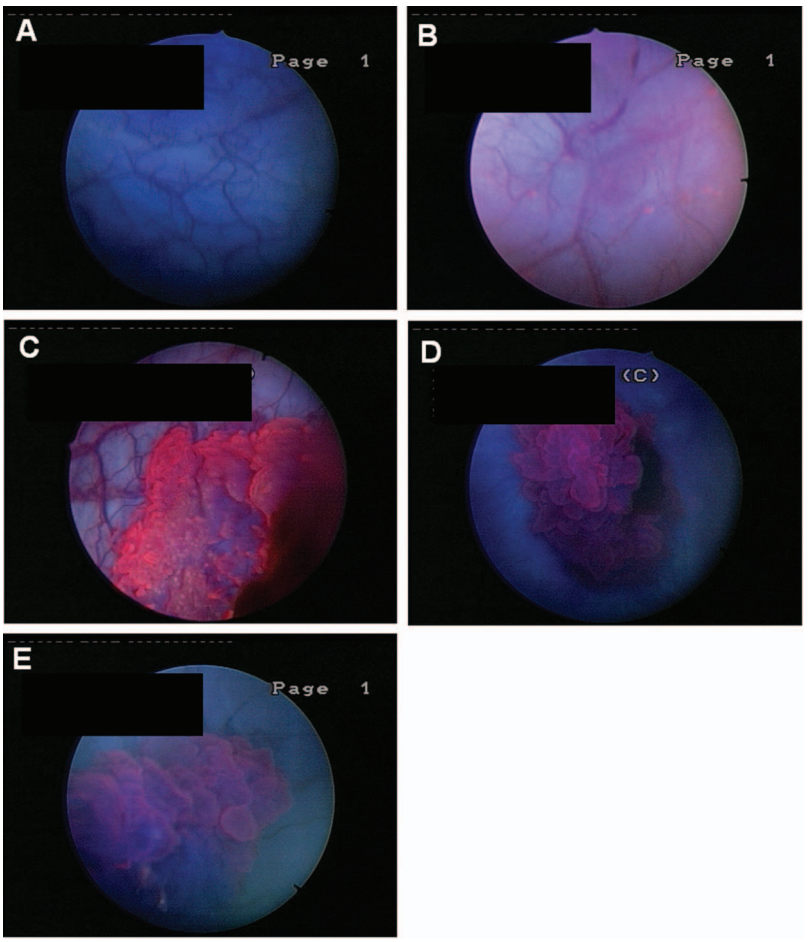

Fig. 3 Representative cystoscopic images of hypericin fluorescence in (a) normal region of the bladder, (b) inflammatory region of the bladder, (c) Grade I TCC, (d) grade II TCC, and (e) grade III TCC showing the differences in fluorescence intensities.

ity and photoreaction using topical hypericin in the bladder as well as other clinically significant short-term side effects such as urinary tract infection.

3.2 *Fluorescence Cystoscopic Imaging and Tumor Detection*

In this study, we assessed the potential of applying image analysis on hypericin fluorescence to grade the bladder cancer *in situ* based on the 58 fluorescent cystoscopic images from the 23 patients. Although the qualitative description of microscopic hypericin fluorescence in *ex vivo* bladder tissue of TCC as well as macroscopic hypericin fluorescence in the detection of CIS had been previously reported in the literature,[16–18] the quantification of hypericin fluorescence for grading of bladder cancer has not yet been reported, to our knowledge. We present our preliminary study with the aim to correlate this fluorescence with the different pathological grades of bladder cancer.

Our previous and current clinical studies have demonstrated that the digitized fluorescence endoscopic system used in this study has the capability of acquiring high-quality images in several milliseconds so as to minimize the effect of hypericin photobleaching and shorten the required time for holding the endoscope steadily. Figure 3 shows representative fluorescence cystoscopic images acquired from normal, inflammatory, and each of the three grades of TCC lesions before any image processing. The fluorescence cystoscopic images showed that suspicious lesions display bright reddish fluorescence, while the surrounding normal bladder mucosa exhibit blue background with no red fluorescence. It was observed that apart from malignant lesions, benign lesions with chronic inflammation also showed reddish fluorescence, i.e., false-positive fluorescence. This may be due to a host of different factors, such as physiological changes in the inflammatory site that also favor the transport and accumulation of hypericin there, the presence of porphyrin and its derivatives from bacteria associated with inflammation at the sites, etc. However, we noticed that the benign lesions with chronic inflammation generally showed milder red fluorescence compared to the TCC cases and that, visually, the fluorescence-positive malignant lesions had significantly higher red-to-blue fluorescence contrast to the surrounding normal tissue as compared to the fluorescence-positive benign lesions.

The images were processed to extract their various colorimetric intensities. After image processing, the intensity of each of the three constituent colors of the fluorescence images, i.e., the red hypericin fluorescence intensity I_R, green autofluorescence I_G, and the backscattered blue excitation light intensity I_B, of the tissue sites of interest was extracted and quantified. The mean intensity values of the 8-bit pixel

Table 2 Comparison of different colorimetric parameters extracted from cystoscopic images of benign and malignant bladder tissue.

Parameters	Benign Tissue	Malignant Tissue
I_R	48.8	76.0
I_B	87.8	82.2
I_G	18.6	17.0
I_R/I_G	2.63±1.92	4.48±1.75
I_R/I_B	0.56±0.37	1.07±0.62

data, i.e., 0 to 255 for each of the three constituent color channels for benign and malignant tissue are shown in Table 2 for comparison. These quantitative intensities concur with our qualitative visual observations that the red fluorescence intensity I_R of malignant tissue (all three grades of TCC) is stronger than that of benign (normal, inflammation, and hyperplasia) tissue. In addition, it is also observed that the diffusely backscattered blue excitation light intensity I_B and the green autofluorescence I_G of malignant tissue is less than that of benign tissue.

Combining all three (red, green, and blue) elements of the clinically valuable fluorescence information, we have chosen both the red-to-green (I_R/I_G) and red-to-blue (I_R/I_B) intensity ratios as appropriate diagnostic intensity ratios to further enhance the colorimetric differences between benign and the different grades of malignant tissue for fluorescence diagnosis. These intensity ratios may provide an indication to the changes in tissue architecture and fluorophore contributions in malignancies. From the intensity ratios, it was found that both the mean I_R/I_G and I_R/I_B values for malignant tissues are generally greater than those of benign tissues. The mean ratio value of I_R/I_G in malignant tissue is 4.48 ± 1.75, which is significantly higher compared to the mean value of 2.63 ± 1.92 in benign tissue (unpaired Student's t-test, $P = 0.00018 < 0.0005$). Similarly, the mean I_R/I_B value of 1.07 ± 0.62 in malignant tissue is also significantly higher than that of 0.56 ± 0.37 in benign tissue (unpaired Student's t-test, $P = 0.00107 < 0.002$).

An interpretation of the observed intensity changes for each of the three color channels with malignancy requires an understanding of the changes in tissue architecture and fluorophore contribution that comes along with carcinoma progression. With the 380 to 450-nm excitation light, the enhanced red fluorescence observed in malignant tissue is mainly due to the photosensitizer-induced fluorescence associated with the selective accumulation of hypericin in malignant lesions, although the endogenous autofluorescence or the presence of porphyrin and its derivatives may have also contributed to the observed red fluorescence, as in cases of bacterial associated inflammation. The green intensity typically represents the intrinsic tissue autofluorescence, and blue intensity largely represents the amount of backscattered light and, to a smaller extent, the blue tissue autofluorescence.

The increase in the red fluorescence intensity for all three grades of malignant TCC over that of benign tissue can be attributed to the greater selective accumulation of hypericin in malignant tissue, possibly due to enhance permeation of the photosensitizer from the tumor vasculature into the tumor interstitial as carried by lipoproteins, coupled with a compromised lymphatic drainage that retards the efflux of hypericin out of tumors. The decrease in green and blue tissue autofluorescence in malignant tissues may be due to the thickening of the epithelial layer, increasing blood volume in the tumor from increase in microvascular density, and decrease in fluorescence quantum yields of endogenous fluorophores, e.g., collagen, elastin, NADH, and flavin. It is known that the fluorescent co-enzymes NADH and FAD, which are important in aerobic metabolism, are normally found in large amounts in normal cells but are absent or expressed in low amounts in anaerobic cancer cells. Besides tissue autofluorescence, the decrease in the diffusely backscattered blue excitation light may be attributed to the increased hemoglobin absorption by a larger blood volume in malignant lesions.[28]

3.3 *Correlation of Colorimetric Intensities with Cancer Grades*

We took the analysis of the intensity ratios a step further and observed that differences in both the I_R/I_G and I_R/I_B intensity ratios were also observed within different grades of malignancies. In fact, these intensity ratios generally exhibit a correlation with cancer malignancy. The statistical means of both intensity ratios decrease with higher grade of bladder cancer. Figure 4 shows the variation of the mean intensity ratios I_R/I_G and I_R/I_B with the three histopathological grades of bladder cancer available in this study in the form of a histogram. The mean intensity ratios for normal and inflammatory conditions are also shown for comparison. From the histogram, it can be seen that a correlation exists between the statistical means of both I_R/I_G and I_R/I_B and the histopathological grade of the bladder cancer tissue and that, specifically, a decrease in both I_R/I_G and I_R/I_B was observed with increasing level of carcinoma differentiation. Using the one-way ANOVA test with one-way analysis of variance for more than three groups of samples, we have determined that statistical differences between five groups of samples, i.e., normal, inflammation, and three different grades of malignant bladder cancer are significant for both the red-to-blue intensity ratio ($P < 0.05$) and the red-to-green intensity ratio ($P < 0.05$). In fact, the P-value for the red-to-blue intensity ratio is 0.0003, and the P-value for the red-to-green intensity ratio is <0.0001. Apart from the observed correlation between the intensity ratios and the histopathological grade of cancer tissue, it is also observed that both the mean intensity ratios of the highest grade of TCC overlap with the hyperplastic inflammatory lesions. As discussed earlier, the fluorescence observed in these inflammatory lesions could be due to many different factors, such as similar physiological changes that are taking place in the inflammatory sites as compared to the carcinoma sites that favor the selective accumulation of hypericin. Such similarities may account for the overlap in the mean intensity ratios, thus resulting in false positives, and may present further implications to the performance of this technique in grading TCC, as discussed in more detail shortly. Nonetheless, our results still highlight the potential of the two diagnostic intensity ratios

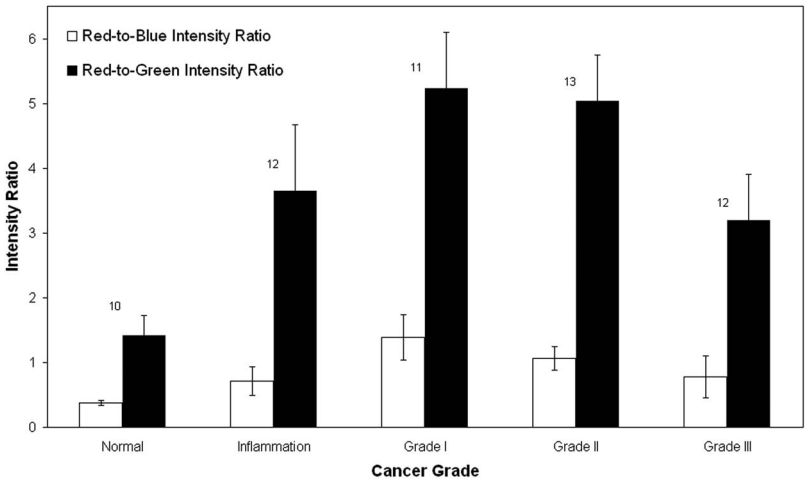

Fig. 4 Comparison of I_R/I_G and I_R/I_B between the three different grades of bladder cancer and benign tissues (normal and inflammation). The number above each bar indicates the sample size for each category of pathology in this study.

based on I_R/I_G and I_R/I_B to discriminate between the different grades of malignant tissue.

Following our earlier statement that an increase in the intensity ratios (due to the higher red intensity and lower autofluorescence intensity) indicates a higher level of hypericin in the tumor, these results seem to intuitively suggest that higher-grade bladder tumors either present a smaller uptake of hypericin during intravesical instillation or a more-effective efflux of hypericin out of the tumors after instillation. However, we attempt to briefly account for the observed correlation based on the alterations in the extracellular matrix in tumors affecting the paracellular transport processes of hypericin through the bladder mucosa and the tissue optics of the excitation light. Previous studies have suggested that the alterations in expression of transmembrane glycoproteins such as cadherins and integrins that mediate the cell-cell and the cell-extracellular matrix adhesion result in modifications in the intercellular adhesion properties of cancer cells during carcinogenesis.[29] Loss of intercellular adhesion during carcinogenesis allows the malignant cells to degrade the cellular matrix for invasion and metastasis according to their aggressiveness. This suggests that the modified histoarchitecture in bladder tumor that arises from the degradation of the extracellular matrix by malignant cells during carcinogenesis may affect the penetration and uptake of hypericin by altering the efficiency of paracellular diffusion of the intravesically instilled hypericin for different grades of bladder cancers. Furthermore, it is also known that the expression of such transmembrane glycoproteins as E-cadherin decreases with decreasing level of differentiation in cell lines.[30]

In relation to our observed results, we propose that the relatively well conserved cellular matrix and tight cellular adhesion due to high level of E-cadherin expression in well-differentiated low-grade bladder cancers may provide barriers to paracellular diffusion of hypericin, which reduces its inward diffusion efficiency during the period of instillation. As the hypericin is taken up by the urothelial cells, their poor diffusion efficiency tends to favor their accumulation at the superficial urothelial region.[18] This urothelial accumulation is also supported in previous studies by Kamuhabwa et al., who observed that despite increasing the instillation times and concentration gradient of hypericin at the surface, the extent of hypericin penetration across the bladder wall was not significantly affected.[31,32] For poorly differentiated high-grade bladder cancers, the largely degraded cellular matrix due to loss of E-cadherin expression facilitates paracellular diffusion of hypericin from the urothelium toward the tumor interior. For this reason, the hypericin taken up by the high-grade urothelial cells has a higher tendency to reach the tumor interior, with a smaller accumulation at the superficial urothelial legion.

Furthermore, as the 440-nm blue excitation light used in this study can penetrate tissue up to a depth of approximately 250 μm,[33] while a typical three to five cell layers thick normal epithelium is approximately 50 μm,[34] this excitation light may be able to excite only the hypericin localized in the superficial urothelium or at most into the submucosa layer (300-μm thick[35]) in normal bladder. For transitional cell carcinoma in which the urothelium thickens to more than 10 cell layers ($>$250 μm),[34] the penetration of the excitation light may be further confined to a limited extent in the urothelium, hence limiting the amount of hypericin that can be excited to the superficial urothelium layer. Hence, the greater accumulation of excitable hypericin in the urothelium of lower-grade bladder cancers due to impeded paracellular transport suggests a possible explanation for their greater fluorescence intensity ratios compared to higher-grade bladder cancers. While the preceding discussion may provide a possible account for our observation, it is also worth noting that such a hypothesis is limited and speculative in nature, and a separate study based on clinical data on glycoprotein expressions and hypericin distribution in clinical biopsies would otherwise provide more valuable insights to our macroscopic observations.

3.4 *Performance of Linear Discriminatory Function in Grading*

The performance of the diagnostic intensity ratios in discriminating between the different grades of malignant tissues were subsequently assessed to determine their sensitivity and speci-

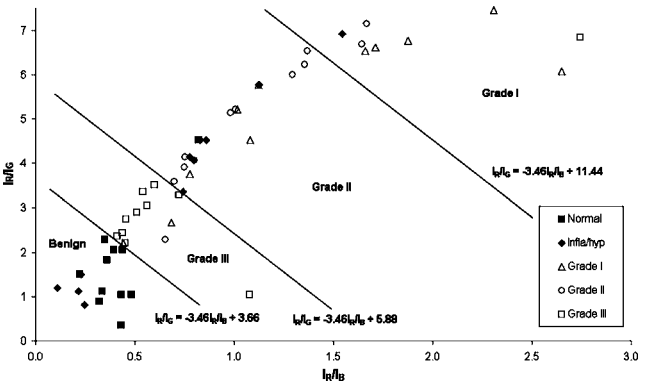

Fig. 5 Two-dimensional scatter map of I_R/I_G versus I_R/I_B for all the image data points in this study. The three diagnostic linear discriminatory functions are also shown, which discriminate the map into four different regions of benign condition and grade I, grade II, and grade III TCC.

ficity in analyzing the grade of bladder cancer *in situ*. Each of the cystoscopic images was mapped onto a two-dimensional (2-D) scatter map based on both its I_R/I_G and its I_R/I_B values, and linear discriminatory functions were developed to discriminate the scatter map into different regions for classification of the lesions in the cystoscopic images into different grades of bladder cancer. Figure 5 shows the 2-D scatter plot of the intensity ratio I_R/I_G with respect to I_R/I_B for all the image data points in this study. Using the developed linear discrimination function that intersected the I_R/I_G axis at 3.66 and I_R/I_B at 1.06, i.e., $I_R/I_G=-3.46I_R/I_B+3.66$, the combined two diagnostic intensity ratios yielded a sensitivity and specificity of 100.0% and 63.6%, respectively, for differentiating malignant from benign tissue. Using the other two developed linear discrimination functions with equations $I_R/I_G=-3.46\ I_R/I_B+5.88$ and $I_R/I_G=-3.46\ I_R/I_B+11.44$, as shown in Fig. 5, we were able to further separate the malignant tissue, i.e., grade III from grade I/II and grade I from grade II/III, respectively. When combined together, these two linear functions were able to separate all three different grades of malignant bladder cancer simultaneously with mean sensitivity and specificity of 68.6% and 86.1%, respectively. The exact level of sensitivity and specificity achieved for classifying each of the different grades of malignant tissue based on all three linear discrimination functions is shown in Table 3. The results obtained from these linear decision lines show that the combination of the two diagnostic intensity ratios can be used to generate possible discriminating criteria that achieve a promising level of sensitivity and specificity grading of bladder cancer *in situ*.

Table 3 Level of sensitivity and specificity achieved in grading the bladder cancer using the developed linear discriminatory functions in the 2-D scatter plot of I_R/I_G versus I_R/I_B.

Histopathological Types	Sensitivity	Specificity
Malignant tissue	100.0%	63.6%
Grade I	45.5%	91.5%
Grade II	76.9%	73.3%
Grade III	83.3%	93.5%

While we have provided possible accounts for our observation on the fluorescence correlation with cancer grade, a clearer understanding of the mechanisms leading to the observed trend warrants a more detailed study. However, for the purpose of this study, we have demonstrated the clinical potential of applying image analysis on hypericin fluorescence cystoscopic images not just to detect malignant lesions from benign surroundings, but also to assist clinicians in further classifying the malignant lesions into different pathological grades *in situ* and in real time based on just the cystoscopic images. Our reported findings based on the application of the three linear discrimination functions on our data set showed that this image analysis technique can produce promising performance on the sensitivity and specificity of detecting each grade of bladder cancer. It is noted from our results that the specificity in classifying each of the three grades of bladder cancer is generally higher compared to the sensitivity in picking up each of the different grades. This is in contrast to the performance achieved in discriminating malignant lesions from benign surroundings where the sensitivity is higher compared to the specificity (Table 3). While a highly sensitive technique may be more desirable for detecting malignant lesions, such a technique with high specificity for classification of different cancer grades will be desirable to ensure an accurate classification of the cancers. Furthermore, it is noted that the specificity in detecting grade II TCC is slightly lower than grade I and grade III TCC, and this may be attributed to its mid-point classification, which makes this category of pathology susceptible to false positives from neighboring categories at both ends. Also, this technique seems to be increasingly more sensitive in detecting higher-grade bladder cancers. As the sample size involved in this study is modest, we note that the results obtained are only approximate indications to the performance of this technique and the actual performance warrants a larger-scale study involving more image data points. A larger study coupled with more complex and refined discrimination functions derived from a larger set of image data points could further fine-tune and improve the sensitivity and specificity performance of this technique.

4 Conclusion

A diagnostic technique capable of performing optical biopsy for noninvasive pathological diagnosis of cancer *in situ* and in real time should prove to be a powerful diagnostic modality in clinical medicine that will likely be a significant clinical advance with considerable impact on patient management. In this clinical study, we highlight the potential of hypericin as a fluorescence marker for optical biopsy. We have shown that a correlation exists between the colorimetric intensity ratios and the grade of bladder cancer and have demonstrated that the application of image analysis techniques on the hypericin fluorescence cystoscopic images has significant potential to grade the bladder cancer *in situ*. The three simple linear diagnostic functions developed based on our modest sample size show promising sensitivity and specificity in classifying the fluorescence cystoscopic images into each of the three patho-

logical cancer grades available in our study. Despite our current results, which show promise for this technique to assist clinicians to diagnose cancer grades in real time, we acknowledge that further studies involving a larger group of patients are still required to truly evaluate the clinical merits of such a technique more conclusively; such clinical trials involving more patients are currently in progress at our center. Furthermore, collection of patient data involving premalignancies such as dysplasia is also currently underway at our center to broaden the scope of this diagnostic technique to include premalignant conditions.

Acknowledgments

This study was supported by the National Medical Research Council and National Cancer Centre Singapore, Singapore.

References

1. A. F. Kantor, P. Hartge, R. N. Hoover, and J. F. Fraumeni, "Epidemiological characteristics of squamous cell carcinoma and adenocarcinoma of the bladder," *Cancer Res.* **48**, 3853–3855 (1998).
2. R. J. Black, F. Bray, J. Ferlay, and D. M. Parkin, "Cancer incidence and mortality in the European Union: Cancer Registry dates and estimates of national incidence for 1990," *Eur. J. Cancer* **33**, 1075–1077 (1990).
3. F. Bray, R. Sankila, J. Ferlay, and D. M. Parkin, "Estimates of cancer incidence and mortality in Europe in 1995," *Eur. J. Cancer* **38**, 99–166 (2002).
4. C. W. S. Cheng, W. K. O. Lau, P. H. Tan, and M. Olivo, "Cystoscopic diagnosis of bladder cancer by intravesical instillation of 5-aminolevulinic acid induced porphyrin fluorescence–the Singapore experience," *Ann. Acad. Med. Singapore* **29**, 153–158 (2000).
5. A. F. Althausen, G. R. Prout, and J. J. Daly, "Noninvasive papillary carcinoma of the bladder associated with carcinoma *in situ*," *Urology* **116**, 575–580 (1976).
6. D. A. Benaron, "The future of cancer imaging," *Cancer Metastasis Rev.* **21**, 45–48 (2002).
7. R. G. Blasberg, "Molecular imaging and cancer," *Mol. Cancer Ther.* **2**, 335–343 (2003).
8. J. K. Dhingra, D. F. Perrault, K. McMillan, E. E. Rebeiz, S. Kabani, R. Manoharan, I. Itzkan, M. S. Feld, and S. M. Shapshay, "Early diagnosis of upper aerodigestive tract cancer by autofluorescence," *Arch. Otolaryngol. Head Neck Surg.* **122**, 1181–1186 (1996).
9. A. Gillenwater, R. Jacob, R. Ganesshappa, B. Kemp, A. El-Naggar, J. Palmer, G. Clayman, M. F. Mitchell, and R. Richards-Kortum, "Noninvasive diagnosis of oral neoplasia based on fluorescence spectroscopy and native tissue autofluorescence," *Arch. Otolaryngol. Head Neck Surg.* **124**, 1251–1258 (1998).
10. R. R. Alfano, D. B. Tata, J. Cordero, P. Tomasheysky, F. W. Longo, and M. A. Alfano, "Laser induced fluorescence spectroscopy from native cancerous and normal tissue," *IEEE J. Quantum Electron.* **20**, 1507–1511 (1984).
11. J. R. Leonard and W. Beck, "Hematoporphyrin fluorescence: an aid in diagnosis of malignant neoplasms," *Laryngoscope* **81**, 365–372 (1971).
12. R. J. Dunn and K. D. Devine, "Tetracycline-induced fluorescence of laryngeal, pharyngeal, and oral cancer," *Laryngoscope* **82**, 189–198 (1972).
13. R. Baumgartner, R. M. Huber, H. Schulz, H. Stepp, K. Rick, F. Gamarra, A. Leberig, and C. Roth, "Inhalation of 5-aminolevulinic acid: a new technique for fluorescence detection of early stage lung cancer," *J. Photochem. Photobiol., B* **36**, 169–174 (1996).
14. F. Koenig, J. Knittel, and H. Stepp, "Diagnosing cancer *in vivo*," *Science* **292**, 1401–1403 (2001).
15. M. Olivo, W. Lau, V. Manivasager, P. H. Tan, and C. Cheng, "Fluorescence confocal microscopy and image analysis of bladder cancer using 5-aminolevulinic acid," *Int. J. Oncol.* **22**, 523–528 (2003).
16. M. Olivo, W. Lau, V. Manivasager, P. H. Tan, K. C. Soo, and C. Cheng, "Macro-microscopic fluorescence of human bladder cancer using hypericin fluorescence cystoscopy and laser confocal microscopy," *Int. J. Oncol.* **23**, 983–990 (2003).
17. M. A. D'Hallewin, P. A. De Witte, E. Waelkens, W. Merlevede, and L. Baert, "Fluorescence detection of flat bladder carcinoma *in situ* after intravesical instillation of hypericin," *J. Urol. (Paris)* **164**, 349–351 (2000).
18. M. A. D'Hallewin, A. R. Kamuhabwa, T. Roskams, P. A. De Witte, and L. Baert, "Hypericin-based fluorescence diagnosis of bladder carcinoma," *Br. J. Urol.* **89**, 760–763 (2002).
19. M. A. D'Hallewin, H. Vanherzeele, and L. Baert, "Fluorescence detection of flat transitional cell carcinoma after intravesical instillation of aminolevulinic acid," *Am. J. Clin. Oncol.* **21**, 223–225 (1998).
20. M. Kriegmair, R. Baumgartner, R. Knuchel, H. Stepp, F. Hofstadter, and A. Hofstetter, "Detection of early bladder cancer by 5-aminolevulinic acid induced porphyrin fluorescence," *J. Urol. (Paris)* **155**, 105–109 (1996).
21. P. Jichlinski, M. Forrer, J. Mizeret, T. Glanzmann, D. Braichotte, G. Wagnieres, G. Zimmer, L. Guillou, F. Schmidlin, P. Graber, H. van den Bergh, and H. J. Leisinger, "Clinical evaluation of a method for detecting superficial surgical transitional cell carcinoma of the bladder by light-induced fluorescence of protoporphyrin IX following the topical application of 5-aminolevulinic: preliminary results," *Lasers Surg. Med.* **20**, 402–408 (1997).
22. W. Zheng, K. C. Soo, R. Sivanandan, and M. Olivo, "Detection of squamous cell carcinoma and precancerous lesions in the oral cavity by quantification of 5-aminolevulinic acid induced fluorescence endoscopic images," *Lasers Surg. Med.* **31**, 151–157 (2002).
23. D. Zaak, D. Frimberger, H. Stepp, S. Wagner, R. Baumgartner, P. Schneede, M. Siebels, R. Knuchel, M. Kriegmar, and A. Hofstetter, "Quantification of 5-aminolevulinic acid induced fluorescence improves the specificity of bladder cancer detection," *J. Urol. (Paris)* **166**, 1665–1669 (2001).
24. S. N. Okpanyi, H. Lidzba, B. C. Scholl, and H. G. Miltenburger, "Genotoxicity of a standardized Hypericum extract," *Drug Dev. Res.* **40**, 851–855 (1990).
25. K. Linde, G. Ramirez, C. D. Mulrow, A. Pauls, W. Weidenhammer, and D. Melchart, "St. John's wort for depression—an overview and meta-analysis of randomized clinical trials," *Br. Med. J.* **313**, 253–258 (1996).
26. W. Zheng, M. Olivo, S. Ranjiv, K. Philip, T. K. Lim, and K. C. Soo, "Endoscopy imaging of 5-ALA-induced PPIX fluorescence for detecting early neoplasms in the oral cavity," *Proc. SPIE* **4597**, 128–132 (2001).
27. H. Stepp, "Fluorescence diagnosis of bladder tumor using 5-aminolevulinic acid–fundamentals and results," in *Physical Principles of Fluorescence Cystoscopy*, R. Baumgartner, M. Kriegmair, and A. Hofstetter, Eds., pp. 16–17, Verlag Endo-Press, Tuttlingen, Germany (2000).
28. R. Richards-Kortum and E. Sevick-Muraca, "Quantitative optical spectroscopy for tissue diagnosis," *Annu. Rev. Phys. Chem.* **47**, 555–606 (1996).
29. K. N. Syrigos, K. J. Harrington, and M. Pignatelli, "Role of adhesion molecules in bladder cancer: an important part of the jigsaw," *Urology* **53**, 428–434 (1999).
30. Z. Popov, S. Gil-Diez de Medina, M. A. Lefrere-Belda, A. Hoznek, S. Bastuji-Garin, and C. C. Abbou, "Low-E-cadherin expression in bladder cancer at the transcriptional and protein level provides prognostic information," *Br. J. Cancer* **83**, 209–214 (2000).
31. A. A. R. Kamuhabwa, I. Cosserat-Gerardin, J. Didelcon, D. Notter, F. Guillemin, T. Roskams, M. A. D'Hallewin, L. Baert, and P. A. M. De Witte, "Biodistribution of hypericin in orthotopic transitional cell carcinomoma bladder tumors: Implication for whole bladder wall photodynamic therapy," *Int. J. Cancer* **97**, 253–260 (2002).
32. A. A. R. Kamuhabwa, T. Roskams, L. Baert, and P. A. M. De Witte, "Microscopic quantification of hypericin fluorescence in an orthotopic rat bladder tumor model after intravesical instillation," *Int. J. Oncol.* **22**, 933–937 (2003).
33. A. J. Welch, J. H. Torres, and W. F. Cheong, "Laser physics and laser-tissue interaction," *Tex Heart Inst. J.* **16**, 141–149 (1989).
34. T. Q. Qie, M. L. Ziedel, and Y. T. Pan, "Detection of tumorigenesis in urinary bladder with optical coherence tomography: optical characterization of morphological changes," *Opt. Express* **10**, 1421–1443 (2002).
35. F. I. Feldchtein, G. V. Gelikonov, V. M. Gelikonov, R. V. Kuranov, and A. M. Sergeev, "Endoscopic applications of optical coherence tomography," *Opt. Express* **3**, 257–270 (1998).